Journal of Inflammation Research Dovepress

Open Access Full Text Article ORIGINAL RESEARCH

Diltiazem Hydrochloride Protects Against Myocardial Ischemia/Reperfusion Injury in a BNIP3L/NIX-Mediated Mitophagy Manner

Xing Zhou[1,*], Quan Lu[2,*], Qiu Wang[2,*], Wenxin Chu[2], Jianhao Huang[2], Jinming Yu[2], Yuechou Nong[2], Wensheng Lu[2,*]

[1]Pharmacy Department, Guangxi Academy of Medical Sciences and the People's Hospital of Guangxi Zhuang Autonomous Region, Nanning, Guangxi, People's Republic of China; [2]Department of Endocrinology and Metabolism, National Key Endocrine Clinical Construction Specialty, Guangxi Academy of Medical Sciences and the People's Hospital of Guangxi Zhuang Autonomous Region, Nanning, Guangxi, People's Republic of China

*These authors contributed equally to this work

Correspondence: Wensheng Lu; Yuechou Nong, Department of Endocrinology and Metabolism, National Key Endocrine Clinical Construction Specialty, Guangxi Academy of Medical Sciences and the People's Hospital of Guangxi Zhuang Autonomous Region, No. 6, Taoyuan Road, Nanning, Guangxi, 530021, People's Republic of China, Email Lwswxqz@163.com; wslu@gxams.org.cn; yuechou_gx@163.com

Background: Mitochondrial calcium uptake-induced mitophagy may play an essential role in myocardial ischemia/reperfusion (MI/R) injury. Diltiazem hydrochloride (DIL), a traditional calcium channel blocker, can alleviate MI/R injury by blocking calcium overload. However, whether the protective mechanism of DIL involves mitophagy remains elusive. This study aimed to clarify the underlying molecular mechanism by which DIL ameliorates MI/R injury by downregulating mitophagy in vivo and in vitro.

Methods: Thirty rats were randomized into three groups: the sham, MI/R, and MI/R+DIL (1 mg/kg) groups (n = 10/per group). MI/R injury was induced by ligating the left anterior descending (LAD) artery for 30 min followed by 60 min of reperfusion in vivo. H9C2 cells were selected to establish an oxygen-glucose deprivation/recovery (OGD/R) model to simulate MI/R injury in vitro. The potential mechanism by which DIL alleviates MI/R injury was analyzed based on tissue morphology, mitophagy-related gene transcription, and protein expression.

Results: According to histological and immunohistochemical evaluations, DIL significantly alleviated myocardial damage in vivo. Moreover, DIL significantly increased cell viability, attenuated OGD/R-induced apoptosis, and inhibited mitochondrial autophagy in vitro. Mechanistically, DIL attenuated mitochondrial autophagy through the upregulation of dual-specificity protein phosphatase 1 (DUSP1) and the downregulation of c-Jun N-terminal kinase (JNK) and Bcl2 interacting protein 3-like (BNIP3L, also known as NIX) expression.

Conclusion: Diltiazem hydrochloride protects against myocardial ischemia/reperfusion injury in a BNIP3L/NIX-mediated mitophagy manner in vivo and in vitro.

Keywords: diltiazem hydrochloride, calcium channel blockers, myocardial infarction, myocardial ischemia/reperfusion injury, mitophagy

Introduction

The coronary atherosclerotic heart disease is the most common fatal cardiovascular disorder, and acute myocardial infarction (AMI) is a major cause of cardiovascular death.[1,2] Rapid restoration of myocardial perfusion after AMI is crucial for maintaining cardiac function; however, reperfusion acts as a double-edged sword which may aggravate myocardial injury, termed myocardial ischemia/reperfusion (MI/R) injury.[3] In recent years, researchers have conducted in-depth explorations of this phenomenon. Heusch et al,[4] Moens et al,[5] and He et al[6] have detailed the various pathophysiological mechanisms that occur during myocardial ischemia-reperfusion, including oxidative stress, inflammatory responses, apoptosis, and mitochondrial dysfunction. Although Bai et al[7] have provided a systematic review of

Received: 7 September 2024
Accepted: 14 November 2024
Published: 16 November 2024

the research on myocardial ischemia-reperfusion injury, the exact mechanisms of MI/R injury have not yet been fully elucidated and deserve further exploration.

Cardiomyocyte death, mainly triggered by a serious shortage of adenosine triphosphate (ATP), is the fundamental pathological outcome of MI/R injury.[8] Mitochondrial oxidative phosphorylation is the major source of ATP in cardiac myocytes.[9] Thus, mitochondrial dysfunction plays a key role in MI/R injury[10,11] Mitochondrial autophagy, also known as "mitophagy", a form of selective mitochondrial autophagy, was first reported in 2005[12] and effectively ensures mitochondrial quality and cell survival.[13,14] Recent studies have revealed that basal mitophagy can effectively eliminate damaged or dysfunctional mitochondria and maintain cellular homeostasis,[15,16] while excessive mitophagy may lead to a low mitochondrial mass, insufficient energy production, and exacerbation of cell damage.[17] Immoderate reactive oxygen species (ROS) production induced by MI/R injury triggers impairment of mitochondrial function, which in turn further activates excessive mitophagy, resulting in impaired mitochondrial ATP production and destruction of cardiomyocyte structure and function.[18] Therefore, excessive mitophagy is a significant pathological feature of MI/R injury. Mitochondrial calcium overload can lead to mitophagy.[19] Downregulation of excessive mitophagy is a key strategy for myocardial salvage.[20] Excessive mitophagy triggered by oxidative stress occurs in a BNIP3L/NIX-dependent manner.[21–23] A high level of mitochondrial ROS caused by MI/R injury promotes the overexpression of the hypoxia-inducible factor HIF-1, resulting in increased expression of the mitophagy receptor BNIP3L/NIX,[24] which then leads to severe mitophagy-induced tissue cell apoptosis.[25] The DUSP1-JNK-BNIP3L/NIX axis has recently been reported to be a possible critical signaling pathway regulating mitophagy.[26–28]

Although the classical calcium channel blocker diltiazem hydrochloride (DIL) markedly inhibits calcium overload and stabilizes the mitochondrial membrane potential, its effect on mitophagy-related MI/R injury remains unclear. Our previous study revealed that DIL significantly reduced myocardial infarction, alleviated MI/R injury and protected cardiomyocytes by promoting the expression of adenine nucleotide transporter-1 (ANT1) and ATPase, inhibiting the expression of caspase-3 and increasing the ratio of Bcl-2/Bax.[29] Therefore, the present study aimed to clarify whether DIL exerts cardioprotective effects against MI/R injury by modulating mitophagy mediated by the DUSP1-JNK-BNIP3L/NIX signaling pathway.

Methods

Ethics Statement

The experimental procedures were conducted per the Operation Rules of the Guangxi People's Hospital Laboratory Center and the Guidelines for the Care and Use of Experimental Animals (NIH Publication No. 85–23, revised in 1996). The study was approved by the Ethics Committee of the People's Hospital of Guangxi Zhuang Autonomous Region (approval no. KY-GZR-2021-100), the Biosafety Committee of the People's Hospital of Guangxi Zhuang Autonomous Region (approval no. KY-GZR-2021-100), and the National Natural Science Foundation of China (approval no. 2021–-45-0266).

Chemicals and Reagents

Unless otherwise specified, all chemicals and reagents were purchased from Sigma–Aldrich (St. Louis, USA).

Animals

Thirty Sprague–Dawley (SD) rats (male; 10–14 weeks old; 200–220 g) were purchased from the Experimental Animal Center of Guangxi Medical University. All animals were housed under standardized conditions (25 ± 2°C, 60 ± 10% humidity, and 12-hour light-dark cycles) and provided food and water ad libitum. The rats were acclimated for at least 14 days before use. The rats were randomly and equally divided into three groups: the sham group (n = 10), MI/R injury group (n = 10), and MI/R+DIL group (n = 10). For the MI/R injury model, rats were subjected to left anterior descending (LAD) coronary artery ligation surgery as previously described [24]. Briefly, all rats were anesthetized with sodium pentobarbital (30 mg/kg, i.p) and placed in the supine position. The rats were intubated with a respiratory tract cannula that was subsequently connected to a small animal ventilator (with a respiration rate of 70 min^{-1}, respiration-to-

expiration ratio of 1:2, and tidal volume of 50 mL/kg; Shanghai Alcott Biotech Co., Ltd., China) for mechanical ventilation. The heart was exposed through the left parasternal incision (between the third and fourth intercostal spaces), and the pericardium was removed. The LAD was ligated with a silk suture for 30 min, and then the suture was loosened to perform myocardial reperfusion for 60 min to establish the MI/R injury model. In the sham group, the LAD was surrounded by a silk thread but not ligated, and saline (2 mL/kg) was injected intravenously 5 minutes before reperfusion. In the MI/R injury group, the rats underwent the abovementioned surgical procedures, and saline (2 mL/kg) was injected intravenously 5 minutes before reperfusion. In the MI/R+DIL group, the rats also underwent the abovementioned surgical procedures, and DIL (1 mg/kg; Jilin Aodong Pharmaceutical Group Yanji Co., Ltd; lot number: B200901) was then injected intravenously 5 min before reperfusion. At the end of the experiment, the animals were immediately sacrificed to obtain myocardial samples.

Histological and Immunohistochemical Analysis

Rat cardiac tissues were fixed with 4% paraformaldehyde for 24 h, dehydrated, embedded in paraffin, and sliced into 4-μm-thick sections. Then, the cardiac sections were stained with hematoxylin and eosin (HE), dehydrated with a graded ethanol series, and finally sealed with a neutral resin for microscopic examination. Immunohistochemistry (IHC) was performed to detect the protein expression of DUSP1, JNK, and BNIP3L/NIX in myocardial tissues. Briefly, the sections were dewaxed, followed by antigen retrieval in citrate buffer (pH = 6). Then, endogenous peroxidase activity and nonspecific binding were blocked with 3% hydrogen peroxide and serum. Next, the sections were incubated with primary antibodies against DUSP1, JNK, and BNIP3L/NIX (1:200, Proteintech, USA) for 1 h at 37°C. After being washed with PBS (0.1 mol/L) three times, the sections were incubated with HRP-labeled secondary antibodies and stained with DAB and hematoxylin (Solarbio, China). Images were captured using a light microscope (Olympus, Tokyo, Japan).

Cell Lines

The rat embryonic cardiomyoblast cell line H9C2 was purchased from ATCC (Rockville, MA, USA). The cells were incubated with Dulbecco's modified Eagle's medium (DMEM, Gibco, USA) comprising 10% fetal bovine serum (FBS, Gibco, USA) and 1% penicillin–streptomycin (Solarbio, China) at 37°C with 5% carbon dioxide. H9C2 cells were used to establish an oxygen–glucose deprivation/recovery (OGD/R) model to simulate MI/R injury in vitro. The OGD/R model was generated as described previously with minor modifications.[25] Briefly, the cells were cultured in DMEM without glucose and serum and placed in an incubator containing 1% O_2, 94% N_2 and 5% CO_2 at 37°C for 6 h. Subsequently, the cells were cultured in complete medium under standard culture conditions (95% O_2, 5% CO_2) at 37°C for 12 h and treated with relevant activators or inhibitors for 12 h. Activators and inhibitors of the DUSP1-JNK-BNIP3L/NIX axis mediating mitophagy are listed in Table 1. In brief, for further experiments, H9C2 cells were divided

Table 1 Activators and Inhibitors of Mitophagy Mediated by the DUSP1-JNK-BNIP3L/NIX Axis

Intervention Strategy	Name (manufacturer)	Working Fluid Concentration	Treating Time
DUSP1			
Activator	Cholera toxin B (CTB) (MCE, USA)	10 μmol/L	12 h
Inhibitor	(E)-2-benzylidene-3-(cyclohexylamino)-2,3-dihydro-1H-inden-1-one (BCI) (MCE, USA)	10 μmol/L	12 h
JNK			
Activator	Anisomycin (Ani) (MCE, USA)	10 μmol/L	12 h
Inhibitor	SP600125 (SP) (MCE, USA)	10 μmol/L	12 h
BNIP3L/NIX			
Activator	4-O-methylascochlorin (MAC) (MCE, USA)	10 μmol/L	12 h
Inhibitor	Bafilomycin A1 (BAF) (Abcam, UK)	10 μmol/L	12 h

Abbreviations: DUSP1, dual-specificity protein phosphatase 1; JNK, c-Jun N-terminal kinase; BNIP3L/NIX, Bcl2 interacting protein 3-like.

into the following groups: the control group, OGD/R model group, OGD/R+DIL group, OGD/R+ activators or inhibitors group, and OGD/R+DIL+ activators or inhibitors group.

Cell Viability and Apoptosis Assay

H9C2 cell viability was tested by the Cell Counting Kit-8 (CCK8, Dojindo, Japan) assay. According to the provided protocol, cells were plated into 96-well plates at a density of 3×10^3 cells per well overnight. After the indicated treatment, 10 μL of CCK-8 solution was added to each well, and the cells were incubated for 1 h (37°C, in 95% air/5% CO2). Finally, the absorbance at 450 nm was detected using a microplate reader. For the cell apoptosis assay, the Annexin V-FITC/PI Apoptosis Detection Kit was used (Keygen Biotech Corp., Ltd., Nanjing, China). The cells were seeded into 6-well plates at a density of 2×10^5 cells/well and cultured overnight in an incubator containing 95% air/5% CO_2 at 37°C. After the indicated treatment, the cells were processed according to the manufacturer's instructions, and the cell apoptosis rate was evaluated by a flow cytometer (Becton Dickinson, NJ, USA).

Mitophagy Assay

H9C2 cells stably expressing mt-Keima were generated via lentivirus infection. H9C2 cells were plated into 24-well plates at a density of 5×104 cells per well 24 h before transfection. After 24 h of infection, the medium containing lentivirus was replaced with normal culture medium. After 24 h, the medium was changed to medium supplemented with 5 μg/mL puromycin, and the infected cells were screened. After the indicated treatment, the mt-Keima fluorescent protein was excited at 440 nm and 586 nm under a confocal laser scanning microscope with fluorescence emission. Additionally, H9C2 cells from each group were collected, fixed in 3% glutaraldehyde for 2 h at 4°C and postfixed with 1% osmium tetroxide for 2 h at 4°C. Then, the fixed samples were gradually dehydrated in a series of dehydration processes: 50%, 70%, and 90% alcohol, 90% alcohol-90% acetone (1:1, v:v), 90% acetone, and 100% acetone. Afterward, the samples were embedded and cut into ultrathin sections. Finally, the mitochondrial autophagosomes in these sections were observed with a transmission electron microscope (JOEL JEM-1010) after the addition of 3% uranium acetate and lead citrate.

Real-Time Quantitative Polymerase Chain Reaction for Detecting Mitophagy-Related Gene Expression

Total RNA was extracted from H9C2 cells using a total RNA extraction kit (ES Science, China). The RNA was reverse transcribed into cDNA using a cDNA synthesis kit (ES Science, China), and the resulting cDNA was amplified by quantitative PCR (ABI Prism 7500 real-time thermocycler) with 2× Super SYBR Green qPCR Master Mix (ES Science, China). β-actin was used as an internal reference gene, and the results were analyzed by the $2^{-\Delta\Delta CT}$ method. The PCR primers used are listed in Table 2.

Table 2 Sequences of Primers Used for Quantitative Real-Time PCR

Gene	Forward Sequence (5′-3′)	Reverse Sequence (5′-3′)
Beclin1	5'-TCAGAGATACCGACTTGTTC-3'	5'-ACTGCCTCCTGTGTCTTCAA-3'
DUSP1	5'-CCGCACAAGATCGACAGACTA −3'	5'-GCGAAGAAGGAGCGACAATC −3'
JNK	5'-AATGGGCACATCACCACTACAC −3'	5'-CGTCTGCGGCTCTTCCTTCA −3'
BNIP3L/NIX	5'-GTCTCACTTAGTCGAGCCGC −3'	5'-TGGAACTCTTTGGGTGGGATG −3'
β-actin	5'-TCCGTGGAGAAGAGCTACGA −3'	5'- GTACTTGCGCTCAGAAGGAG −3'

Abbreviations: PCR, polymerase chain reaction; DUSP1, dual-specificity protein phosphatase 1; JNK, c-Jun N-terminal kinase; BNIP3L/NIX, Bcl2 interacting protein 3-like.

Protein Isolation and Western Blot Analysis

Total protein was extracted from H9C2 cells using RIPA lysis buffer supplemented with protease inhibitor (Solarbio, Beijing, China), and the protein concentration was measured with a BCA protein assay kit (Beyotime, Shanghai, China). The proteins were separated by sodium dodecyl sulfate–polyacrylamide gel electrophoresis (SDS–PAGE) (Thermo Fisher Scientific, USA) and transferred to PVDF membranes. The membranes were blocked with 5% skim milk for 2 h at room temperature and then incubated with the following primary antibodies at 4°C overnight: rabbit anti-DUSP1, JNK, BNIP3L/NIX, Beclin1 and LC3II (Proteintech, USA). After washing with TBST, the membranes were incubated with a horseradish peroxidase-conjugated anti-rabbit IgG secondary antibody (Proteintech, USA) for 2 h at room temperature. The membranes were developed using an enhanced luminescence (ECL) kit (Affinity), and images were obtained by fluorescence imaging using an ODYSSEY® CLx Infrared Imaging System (LI-COR Odyssey CLx, USA). GAPDH was used as an internal reference.

Statistical Analysis

Al the data are presented as the mean ± standard deviation (SD). One-way ANOVA was used to compare the differences between groups. The post-hoc test selected was Tukey's HSD test. Additionally, repeated measures ANOVA was used to analyze cell viability measurements. Data analyses were performed with the SPSS 26.0 statistical software package (IBM Corp., Armonk, NY, USA). Statistical significance was set at the $P < 0.05$ level.

Results

DIL Significantly Ameliorated Myocardial Damage by Upregulating DUSP1 and Downregulating JNK and BNIP3L/NIX in vivo

Hematoxylin and eosin (HE) staining was utilized to identify cardiac tissue damage, as shown in Figure 1A. There were no visible signs of myocardial tissue injury in the sham group, and the myocardial infrastructure was normal. In contrast, the MI/R group exhibited marked myocardial injury, as evidenced by a disorder of the muscle fibers, swelling, necrosis, hemorrhage, and increased infiltration of focal inflammatory cells. Nevertheless, DIL reversed these pathological changes in the MI/R+DIL group. Subsequently, the protein expression levels of DUSP1, JNK and BNIP3L/NIX in cardiac sections from the three groups were examined using IHC staining (Figure 1B). Compared with that in the sham group, the protein expression of DUSP1 was significantly decreased in the MI/R group ($P < 0.01$) (Figure 1C); moreover, the protein expression of JNK (Figure 1D) and BNIP3L/NIX was significantly increased ($P < 0.01$) (Figure 1E). Remarkably, these trends could be reversed by DIL in the MI/R+DIL group ($P < 0.01$). The above HE and IHC experimental evidence showed that DIL protected myocardial tissue against MI/R injury by upregulating DUSP1 expression and downregulating JNK and BNIP3L/NIX expression in vivo.

DIL Increased Myocardial Cell Viability and Inhibited Apoptosis by Attenuating OGD/R-Induced Mitophagy in vitro

H9C2 cells were used to establish an OGD/R model to simulate MI/R injury in vitro (Figure 2A). In the control group, the H9C2 cells exhibited long or short spindle shapes with neat edges and good growth. However, the morphology of H9C2 cells was irregular, and the cell growth rate significantly decreased in the OGD/R group. Compared with those in the OGD/R group, the defects in the morphology and growth rate of H9C2 cells in the OGD/R+DIL group were improved by DIL intervention. The changes in the activity of H9C2 cells treated with DIL at different concentrations (10^{-7} M, 10^{-6} M, or 10^{-5} M) over time (6 h, 12 h, or 24 h) are presented in Figure 2B. Cell viability was lower in the OGD/R group than in the control group ($P < 0.01$). Compared with those in the OGD/R group, the viability of cells in the OGD/R+DIL group treated with different concentrations of DIL was significantly greater ($P < 0.05$). At the same DIL concentration, the cell survival rate was greatest after 12 h of treatment. In parallel, after the same intervention time, H9C2 cells treated with 10^{-6} M DIL exhibited the highest survival rate. Therefore, treatment with 10^{-6} M DIL for 12 h was selected as the optimal intervention condition for subsequent experiments. Then, the effect of treatment with 10^{-6} M DIL for 12 h on the apoptosis of OGD/R-treated H9C2 cells was examined. The results of the apoptosis assay are shown in Figure 2C and D. Compared with that in the control group, the apoptosis rate in the OGD/R group was

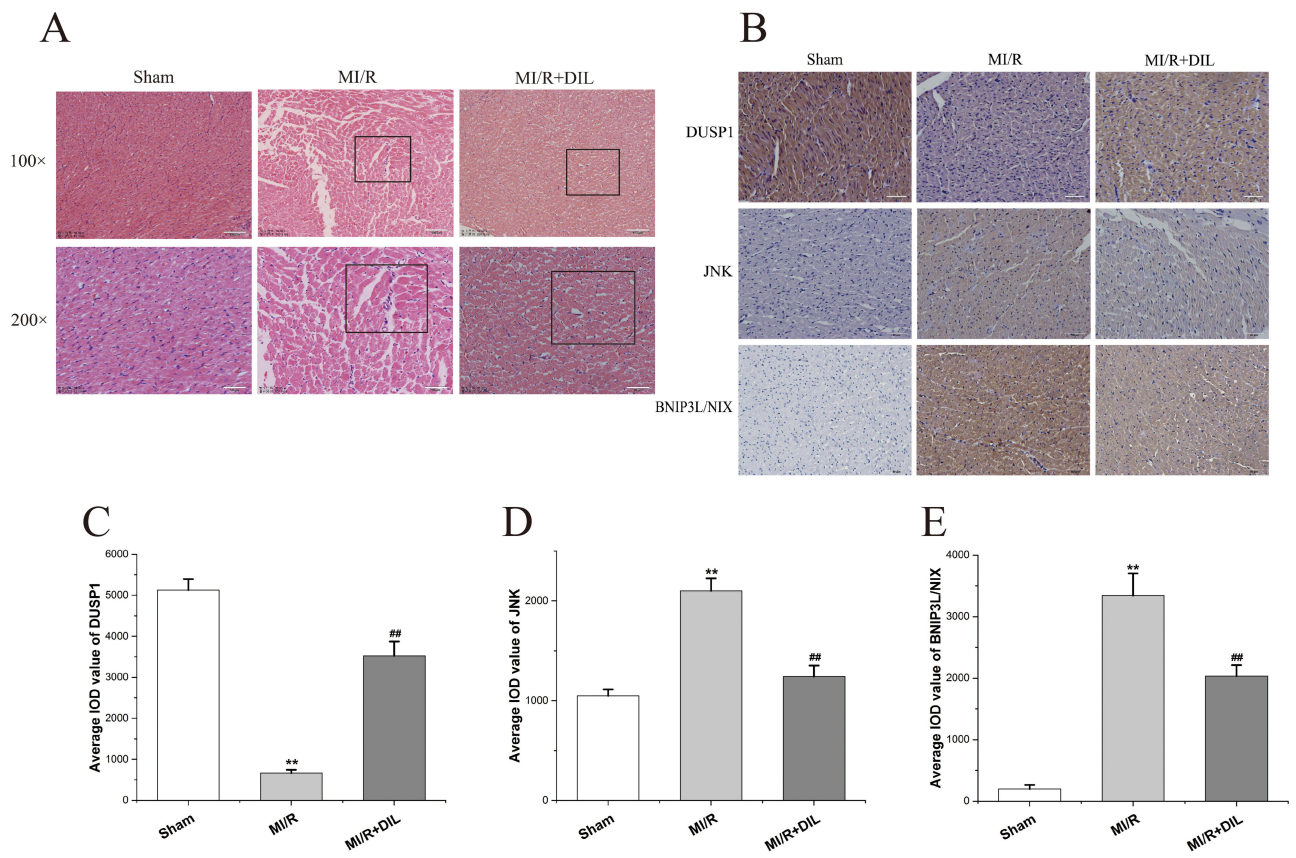

Figure 1 The effects of DIL on histological and immunohistochemical analyses of cardiac muscular tissue in rats with MI/R injury. (**A**) Hematoxylin and eosin (HE) staining of cardiac muscular tissue in the three groups. Original magnification: ×100, scale bar = 100 μm (upper row); ×200, scale bar = 50 μm (lower row). (**B**) Representative images of immunohistochemical (IHC) staining of DUSP1, JNK, and BNIP3L/NIX in the three groups. (**C**–**E**) Comparison of the average IOD values of DUSP1, JNK, and BNIP3L/NIX expression in myocardial tissue among the three groups determined by IHC analysis. $^{**}P < 0.01$ relative to the sham group, $^{\#\#}P < 0.01$ relative to the MI/R group.

significantly greater ($P < 0.01$). In particular, this effect was partly reversed by DIL intervention ($P < 0.01$). These results indicated that DIL could significantly increase cell activity and inhibit OGD/R-induced apoptosis.

Mitophagy is considered to be closely associated with mitochondrial homeostasis.[30] To clarify the effects of DIL on mitophagy in MI/R injury, H9C2 cells were stably transfected with mt-Keima, which is a good indicator of mitophagy flux (Figure 3). mt-Keima emits neutral green fluorescence (440 nm) as a base for mitophagy under normal conditions but exhibits acidic red fluorescence (586 nm) as an excessive mitophagy signal.[31] The OGD/R injury model showed a marked increase in bright red puncta (acidic mitochondria) in H9C2 cells, suggesting excessive mitophagic flux. However, DIL intervention restored the number of neutral mitochondria, indicating that DIL could inhibit excessive mitophagy. Furthermore, autophagosomes were observed using transmission electron microscopy (TEM) (Figure 4). The control group exhibited normal mitochondrial morphology, while more autophagosomes were detected in the OGD/R group. In contrast, DIL intervention significantly reduced the number of autophagosomes in the OGD/R+DIL group. The above results showed that the calcium channel blocker DIL protected H9C2 cells from MI/R injury by restraining mitophagy.

DIL Inhibited Excessive Mitophagy Through the DUSP1-JNK-BNIP3L/NIX Pathway in vitro

The results of the RT–qPCR analyses are displayed in Figure 5. Compared to those in the control group, the expression levels of Beclin 1, JNK and BNIP3L/NIX were significantly greater in the OGD/R group, but only DUSP1 expression was significantly lower (all $P < 0.01$). Remarkably, this effect could be reversed by DIL intervention (all $P < 0.01$). Consistent with the RT–qPCR results, the Western blot results also indicated significantly increased protein expression of Beclin 1, LC3B, JNK and BNIP3L/NIX and decreased DUSP1 protein expression in the OGD/R group compared to the

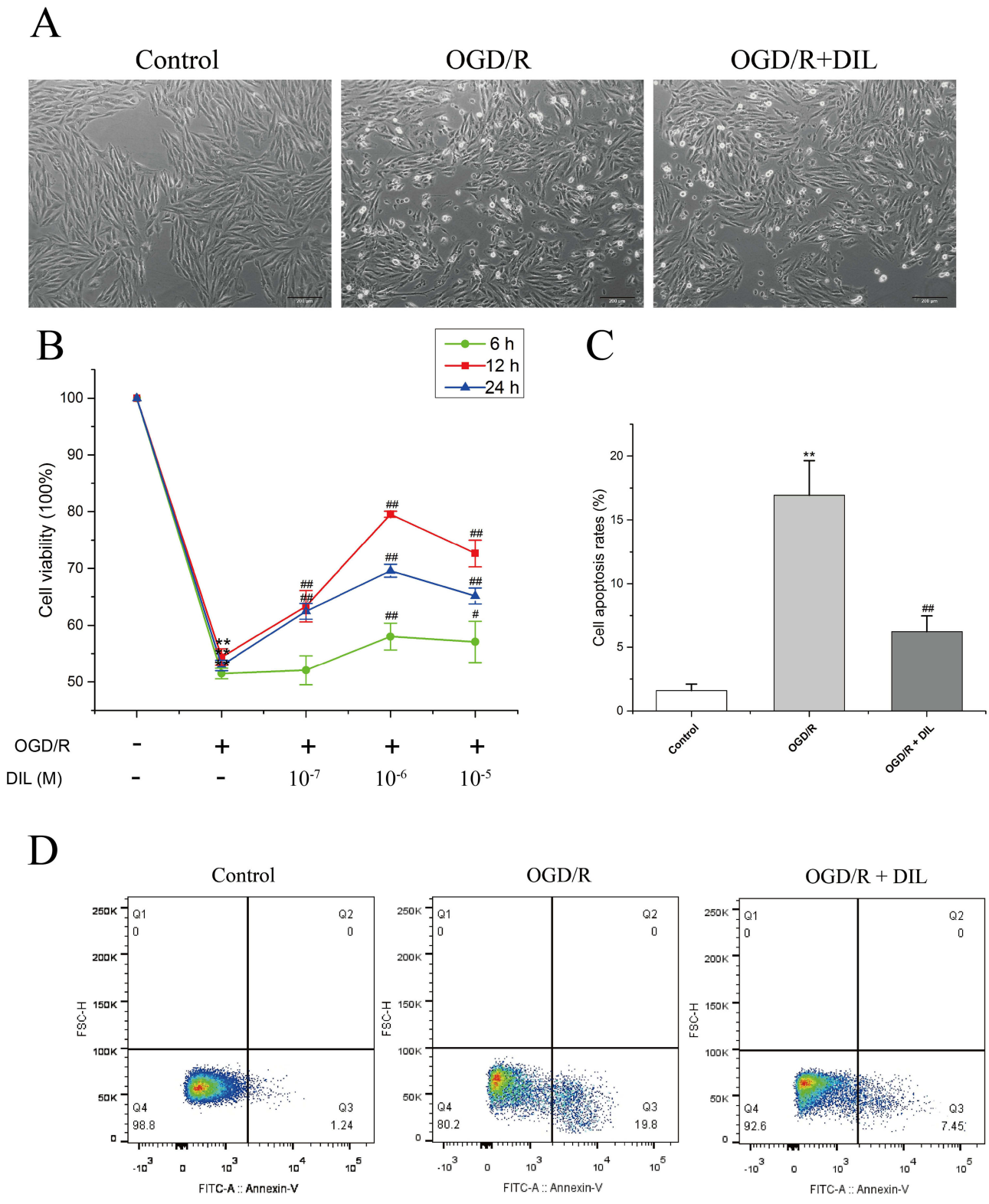

Figure 2 Effect of DIL intervention on cell viability and the apoptosis rate. (**A**) Morphological characteristics and growth status of H9C2 cells in the control, OGD/R, and OGD/R + DIL groups (×200). (**B**) Viability of H9C2 cells treated with different concentrations of DIL for different durations in the control, OGD/R, and OGD/R + DIL groups. (**C** and **D**) The apoptosis rates of H9C2 cells in the control, OGD/R, and OGD/R + DIL groups were assessed by Annexin V-FITC/PI staining. **P < 0.01 relative to the control group, ##P < 0.01 relative to the OGD/R group.

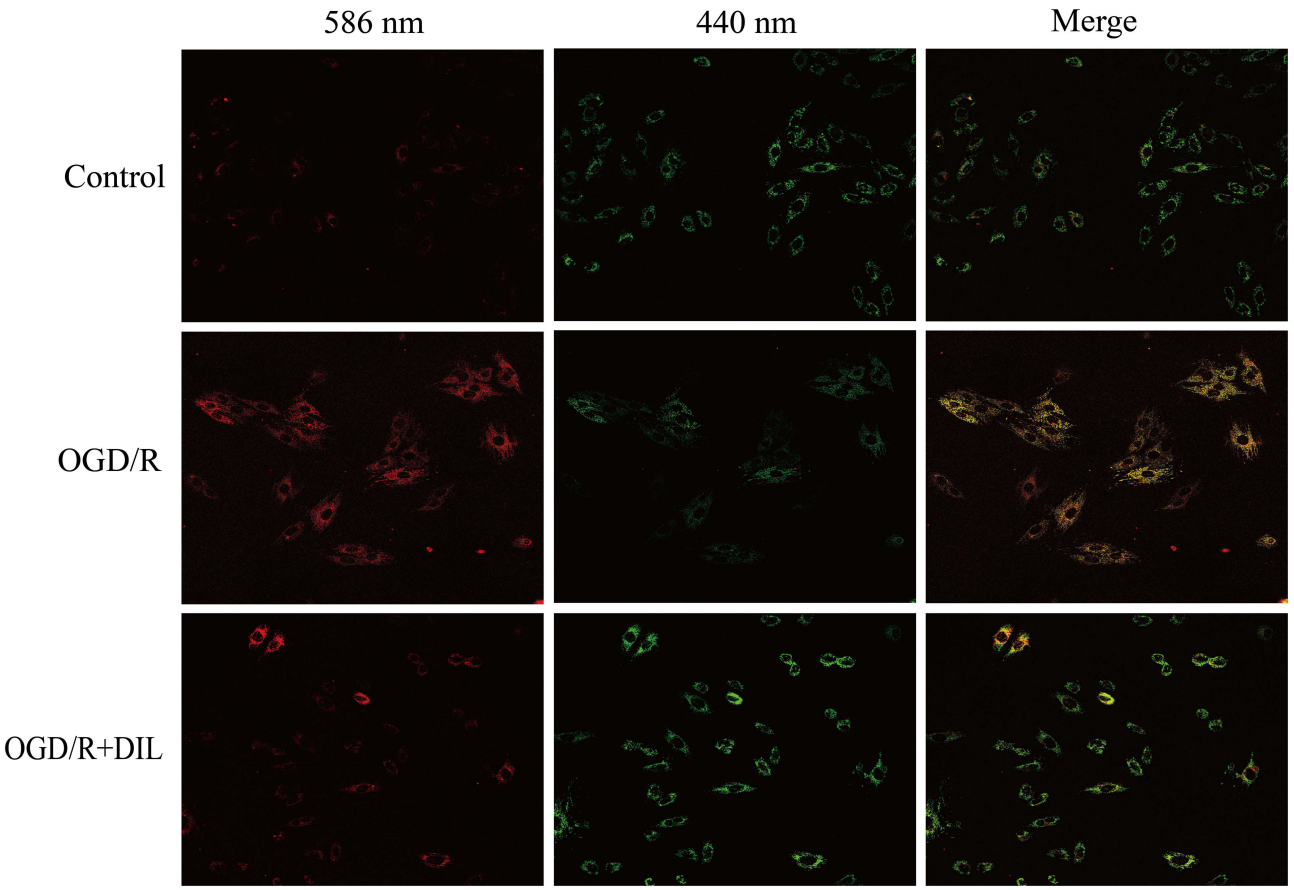

Figure 3 Mt-Keima showing normal mitochondria (green) and mitochondria in autophagosomes (red) in H9C2 cells. H9C2 cells stably expressing mt-Keima were generated via lentivirus infection in the control, OGD/R, and OGD/R + DIL groups. The mt-Keima fluorescent protein was excited at 440 nm and 586 nm under a confocal laser scanning microscope, and fluorescence emission was detected in the three groups. Scale bar, 100 μm.

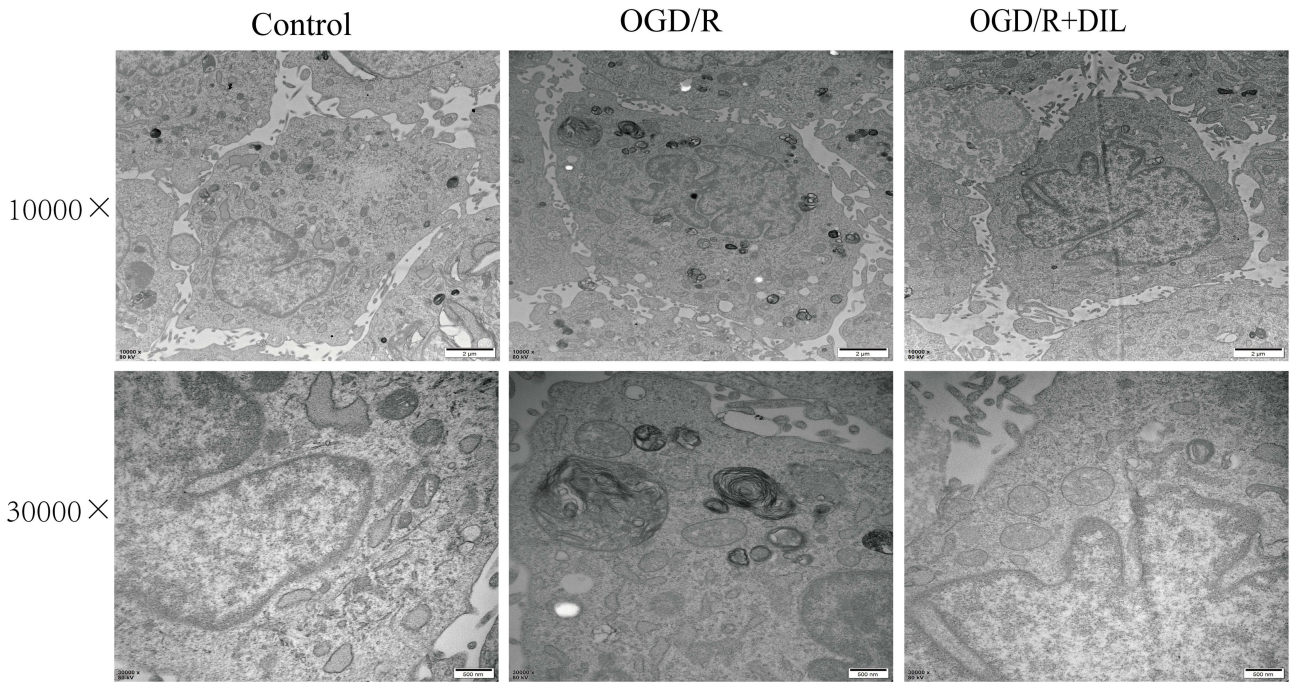

Figure 4 The mitochondrial autophagosomes were observed under a transmission electron microscope (TEM). The morphology of mitochondria and autophagosomes in the control, OGD/R and OGD/R + DIL groups in vitro was observed via transmission electron microscopy (TEM). Original magnification: ×10000, scale bar = 2 μm (upper row); ×30000, scale bar = 500 nm (lower row).

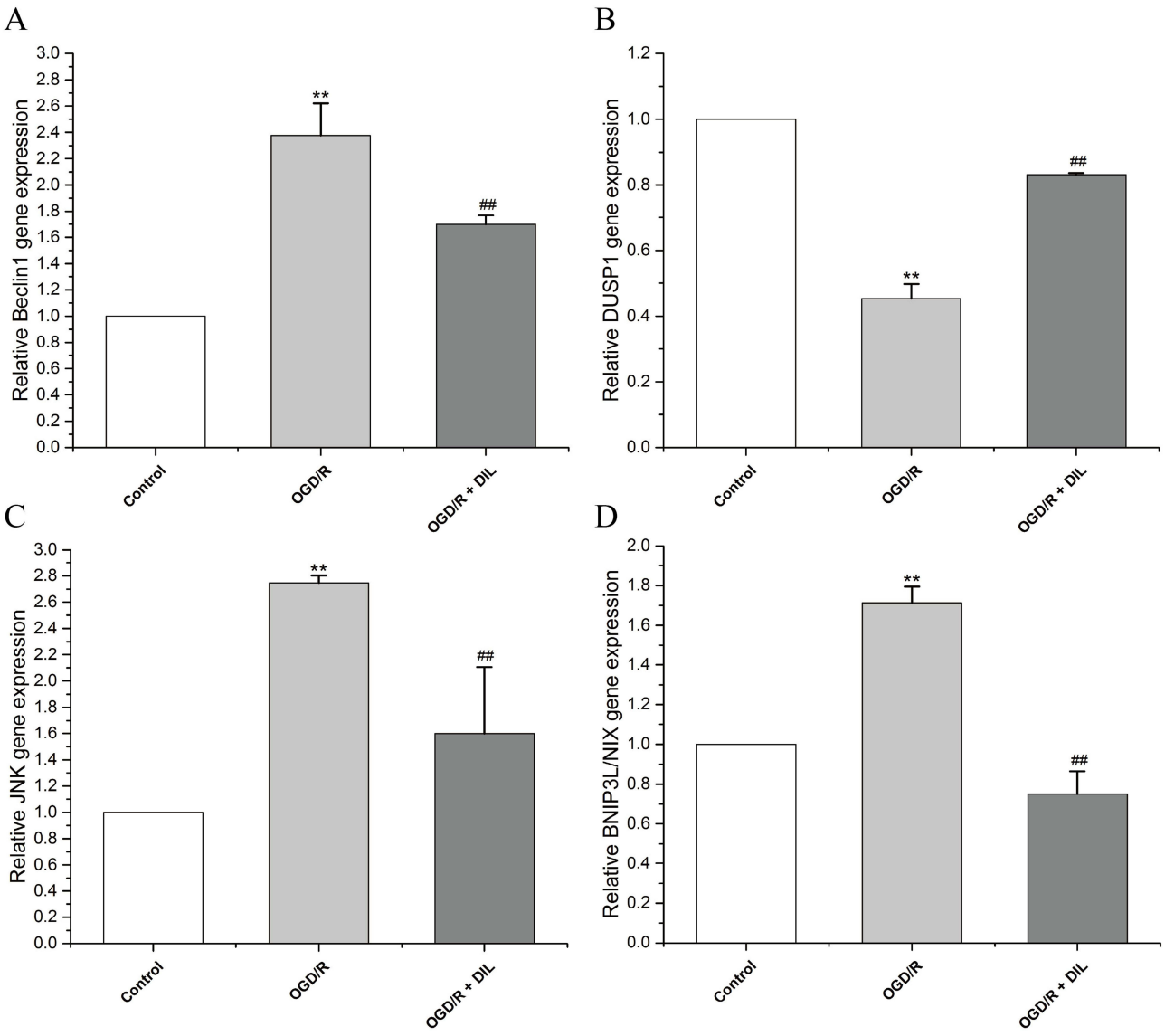

Figure 5 RT–qPCR analysis of the mRNA levels of Beclin 1, DUSP1, JNK, and BNIP3L/NIX in the control, OGD/R, and OGD/R + DIL groups. Compared to those in the control group, the expression levels of Beclin 1 (**A**), JNK (**C**) and BNIP3L/NIX (**D**) were significantly greater in the OGD/R group, but only DUSP1 expression (**B**) was significantly lower (all P < 0.01). Remarkably, this effect could be reversed by DIL intervention (all P < 0.01). **P < 0.01 relative to the control group; ##P < 0.01 relative to the OGD/R group.

control group. As anticipated, DIL intervention reversed these changes (all $P < 0.05$) (Figure 6). These results revealed that DIL protected H9C2 cells against MI/R injury at the gene transcription and protein translation levels, suggesting a novel mechanism by which the calcium channel blocker DIL alleviates myocardial ischemia/reperfusion injury by regulating mitophagy-related gene expression.

Additionally, the results of RT–qPCR and Western blot assays with activators/inhibitors of DUSP1, JNK and BNIP3L/NIX are displayed in Figures 7 and 8. Compared with that in the OGD/R group, the DUSP1 gene expression level was significantly upregulated in the OGD/R+DIL and OGD/R+CTB (an activator of DUSP1) groups ($P < 0.01$). Moreover, the DUSP1 expression level was significantly downregulated in the OGD/R+BCI (an inhibitor of DUSP1) group ($P < 0.01$), and these changes were reversed by DIL in the OGD/R+BCI+DIL group ($P < 0.01$) (Figure 7A and 8A and B). Additionally, Ani (an activator of JNK) significantly upregulated JNK expression in the OGD/R+Ani group ($P < 0.01$). However, DIL and SP (an inhibitor of JNK) significantly downregulated JNK expression in the OGD/R+DIL and OGD/R+SP groups compared with that in the OGD/R group ($P < 0.01$). Unexpectedly, compared with that in the OGD/R

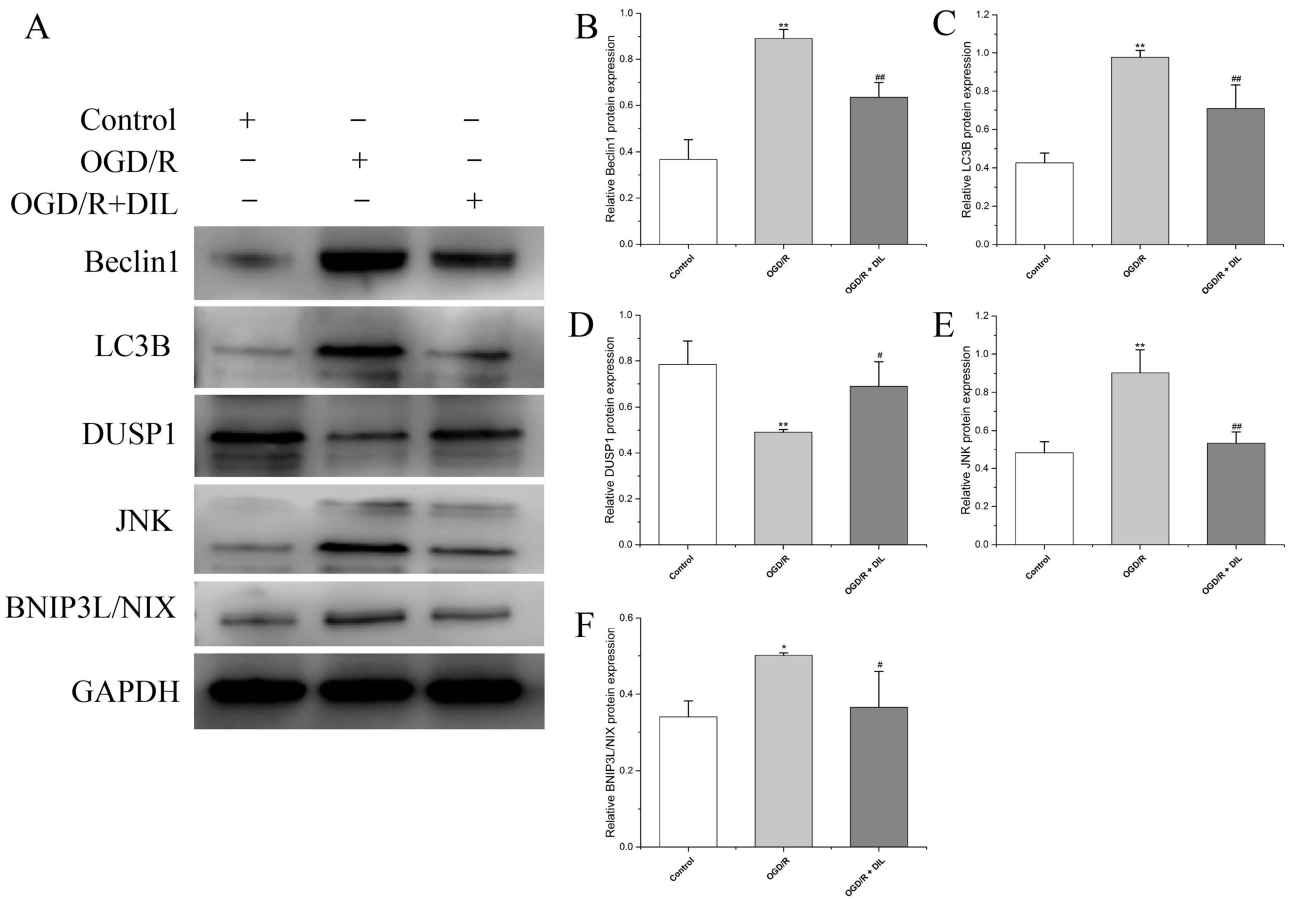

Figure 6 Western blot analyses of the Beclin 1, LC3B, DUSP1, JNK, and BNIP3L/NIX proteins in the control, OGD/R, and OGD/R + DIL groups. (**A**) The electrophoresis results of mitophagy-related proteins from the Western blot. The analyses indicated significantly increased protein expression of Beclin 1 (**B**), LC3B (**C**), JNK (**E**), and BNIP3L/NIX (**F**) and decreased DUSP1 protein expression (**D**) in the OGD/R group compared to the control group. DIL intervention reversed these changes (all $P < 0.05$). *$P < 0.05$, **$P < 0.01$ relative to the control group; $^{\#}P < 0.05$, $^{\#\#}P < 0.01$ relative to the OGD/R group.

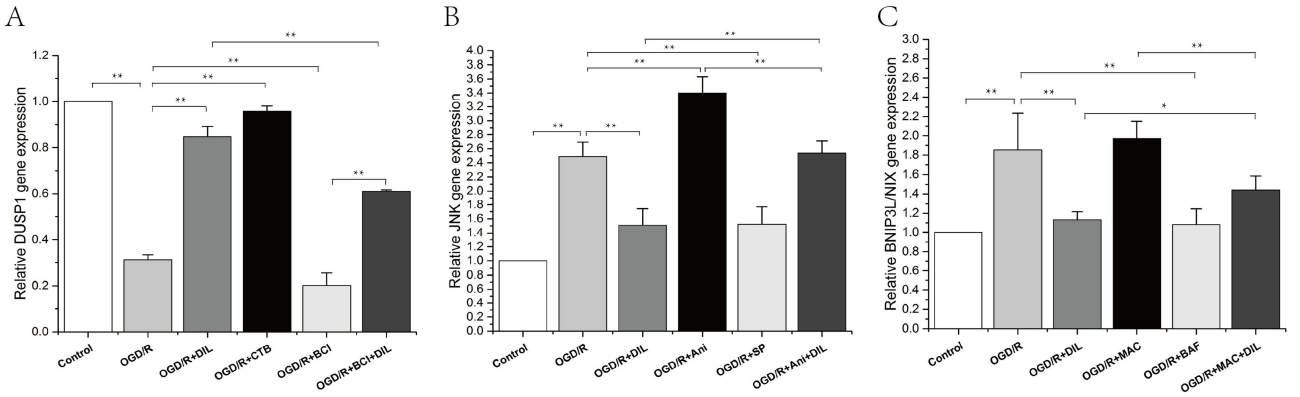

Figure 7 RT–qPCR analysis of the mRNA levels of the DUSP1, JNK, and BNIP3L/NIX genes after treatment with DUSP1, JNK, and BNIP3L/NIX inhibitors or activators in the different groups. (**A**) The DUSP1 expression level was significantly decreased in the OGD/R+BCI (an inhibitor of DUSP1) group ($P < 0.01$), and these changes were reversed by DIL in the OGD/R+BCI+DIL group ($P < 0.01$). (**B**) Ani (an activator of JNK) significantly upregulated JNK expression in the OGD/R+Ani group ($P < 0.01$). However, DIL and SP (an inhibitor of JNK) significantly downregulated JNK expression in the OGD/R+DIL and OGD/R+SP groups compared with that in the OGD/R group ($P < 0.01$). Unexpectedly, compared with that in the OGD/R+Ani group, the JNK expression level did not increase further under DIL intervention but obviously decreased in the OGD/R+Ani+DIL group ($P < 0.01$), which indicated that DIL-induced DUSP1 partly inhibited JNK expression. (**C**) MAC (an activator of BNIP3L/NIX) significantly upregulated BNIP3L/NIX expression in the OGD/R+MAC group. Compared with that in the OGD/R+DIL or OGD/R+BAF (an inhibitor of BNIP3L/NIX) group, BNIP3L/NIX expression in the OGD/R+DIL or OGD/R+BAF group was significantly lower in the DIL and BAF groups ($P < 0.01$). Moreover, compared with that in the OGD/R +MAC group, the BNIP3L/NIX expression level did not increase further under DIL intervention but obviously decreased in the OGD/R+ MAC+DIL group ($P < 0.01$), which indicated that DIL-induced DUSP1 partly inhibited BNIP3L/NIX expression. The data are presented as the means ± SDs of three independent experiments performed in duplicate. *$P < 0.05$, **$P < 0.01$.

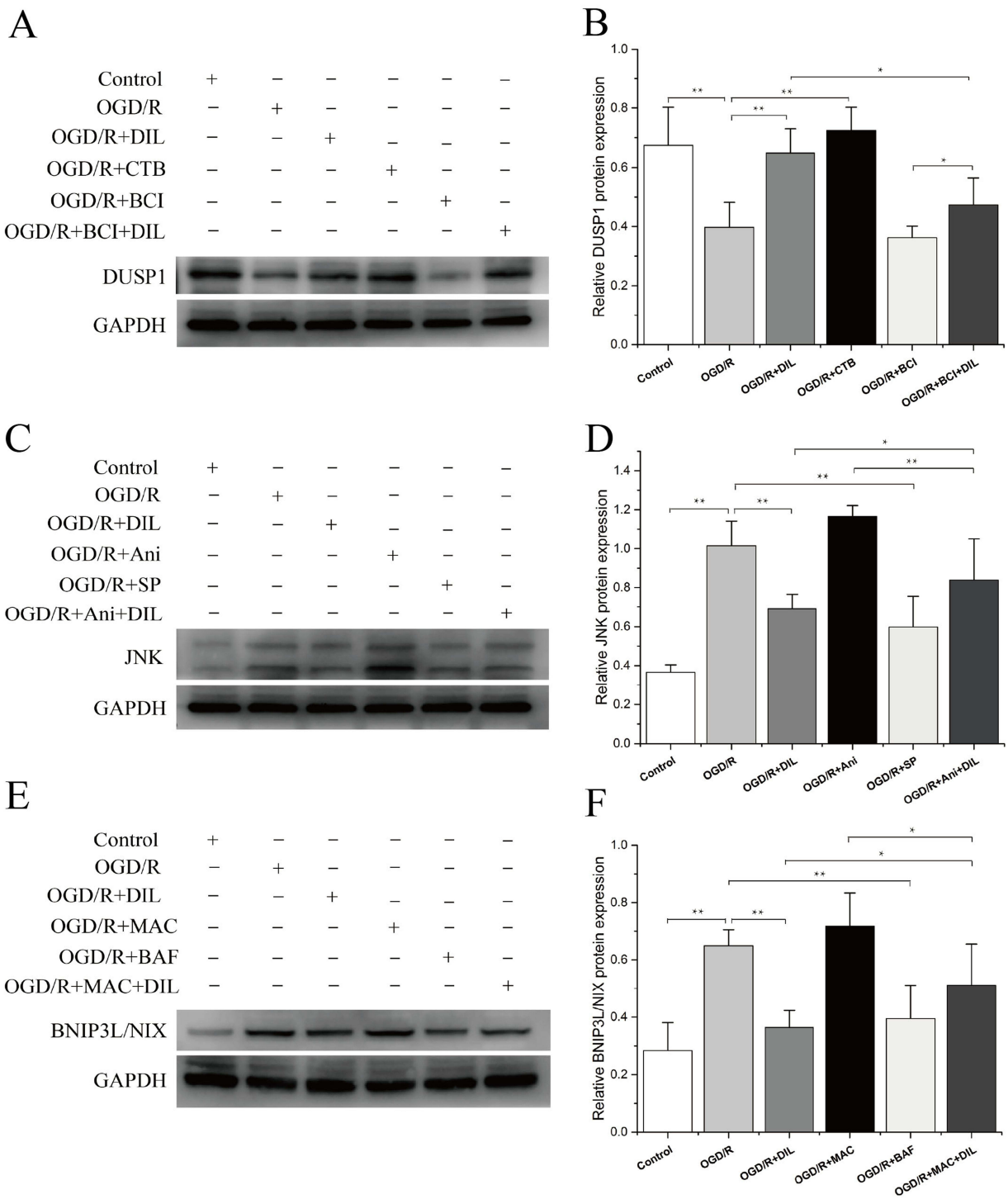

Figure 8 Western blot analyses of DUSP1, JNK, and BNIP3L/NIX after treatment with DUSP1, JNK and BNIP3L/NIX inhibitors or activators in the different groups. (**A** and **B**) Compared with that in the OGD/R group, the DUSP1 gene expression level was significantly upregulated in the OGD/R+DIL and OGD/R+CTB (an activator of DUSP1) groups ($P < 0.01$). Moreover, the DUSP1 expression level was significantly decreased in the OGD/R+BCI (an inhibitor of DUSP1) group ($P < 0.01$), and these changes were reversed by DIL in the OGD/R+BCI+DIL group ($P < 0.01$). (**C** and **D**) Ani (an activator of JNK) significantly upregulated JNK expression in the OGD/R+Ani group ($P < 0.01$). However, DIL and SP (an inhibitor of JNK) significantly downregulated JNK expression in the OGD/R+DIL and OGD/R+SP groups compared with that in the OGD/R group ($P < 0.01$). Unexpectedly, compared with that in the OGD/R+Ani group, the JNK expression level did not increase further under DIL intervention but obviously decreased in the OGD/R+Ani+DIL group ($P < 0.01$), which indicated that DIL-induced DUSP1 partly inhibited JNK expression. (**E** and **F**) MAC (an activator of BNIP3L/NIX) significantly upregulated BNIP3L/NIX expression in the OGD/R+MAC group. Compared with that in the OGD/R+DIL or OGD/R+BAF (an inhibitor of BNIP3L/NIX) group, BNIP3L/NIX expression in the OGD/R+DIL or OGD/R +BAF group was significantly lower in the DIL and BAF groups ($P < 0.01$). Moreover, compared with that in the OGD/R+MAC group, the BNIP3L/NIX expression level did not increase further under DIL intervention but obviously decreased in the OGD/R+ MAC+DIL group ($P < 0.01$), which indicated that DIL-induced DUSP1 partly inhibited BNIP3L/NIX expression. The data are presented as the means ± SDs of three independent experiments performed in duplicate. *$P < 0.05$, **$P < 0.01$.

+Ani group, the JNK expression level did not increase further under DIL intervention but obviously decreased in the OGD/R+Ani+DIL group ($P < 0.01$), which indicated that DIL-induced DUSP1 partly inhibited JNK expression (Figures 7B and 8C and D). Furthermore, MAC (an activator of BNIP3L/NIX) significantly upregulated BNIP3L/NIX expression in the OGD/R+MAC group. Compared with that in the OGD/R+DIL or OGD/R+BAF (an inhibitor of BNIP3L/NIX) group, BNIP3L/NIX expression in the OGD/R+DIL or OGD/R+BAF group was significantly lower in the DIL and BAF groups ($P < 0.01$). Moreover, compared with that in the OGD/R+MAC group, the BNIP3L/NIX expression level did not increase further under DIL intervention but obviously decreased in the OGD/R+ MAC+DIL group ($P < 0.01$), which indicated that DIL-induced DUSP1 partly inhibited BNIP3L/NIX expression (Figure 7C and 8E and F). These results revealed that mitophagy-related gene expression was regulated via the DUSP1-JNK-BNIP3L/NIX pathway.

Discussion

The current study demonstrated that DIL significantly decreased myocardial damage in this rat model of MI/R injury in vivo. Exposure to DIL decreased mitophagy, significantly decreased OGD/R-induced apoptosis, and improved H9C2 cell viability in vitro. Moreover, the mechanism underlying the protective effect of DIL on cardiac cells involves the modulation of the DUSP1-JNK-BNIP3L/NIX-related mitophagy pathway. To the best of our knowledge, this is the first work investigating how DIL is shielded from MI/R damage by inhibiting mitophagy.

MI/R is associated with clinical interventions such as percutaneous coronary intervention (PCI) or thrombolytic therapy, which can relieve myocardial ischemia but also cause further injury, known as MI/R injury.[32] The pathogenesis of MI/R injury is complex and intricate and involves multifactorial mechanisms, including excess inflammatory responses, oxidative stress, intracellular calcium overload, iron accumulation, impaired mitochondrial function, and microcirculatory disturbance. Clinically, it manifests as the expansion of the myocardial infarct area, contractile dysfunction, heart failure and sudden death.[33] In this study, MI/R injury was induced by 30 min of coronary ischemia followed by 60 min of reperfusion in vivo. Our present findings demonstrated that MI/R causes cardiac function impairment and severe myocardial damage, manifested as myofibrillar disarray, swelling, necrosis, hemorrhage and focal inflammatory infiltrates, but DIL can protect against MI/R injury.[34] Furthermore, OGD/R decreased cell viability and apoptosis in vitro, but these effects were partly reversed by DIL treatment. These results are consistent with those of previous studies.[35]

A growing body of evidence has suggested that mitophagy is an important mechanism for MI/R injury. Excessive mitochondrial ROS production caused by MI/R injury may destroy mitochondria and subsequently cause hyperactivation of autophagy, the consequences of which are further deterioration of mitochondrial number and mitochondrial density, resulting in further deterioration of cardiac structure and function. Therefore, the downregulation of abnormal excessive mitophagy is considered an important target for protection against MI/R injury.[36]

Beclin1 is a key molecule in the formation of autophagosomes[37,] and LC3-II levels are correlated with the number of autophagosomes.[38] MI/R induces oxidative stress through an increase in oxygen free radicals, and then oxidative stress can induce autophagy by upregulating the expression of the autophagy-related proteins LC3 and Beclin1.[39–41] Furthermore, our previous study revealed that DIL increased the protein expression of the antiapoptotic protein Bcl-2 in a rat model of MI/R injury. BNIP3 and NIX are homologous members of the Bcl-2 family of proteins;[42] thus, it was suggested that DIL affects mitophagy mediated by BNIP3L/NIX. BNIP3L/NIX is also a mitophagy receptor strongly associated with MI/R. Under physiological conditions, BNIP3L/NIX interacts directly with mitochondrial LC3-II to form mitophagy receptors, which mediate mitophagy initiation and facilitate the removal of damaged mitochondria. However, MI/R injury induces BNIP3L/NIX overexpression, which triggers excessive mitophagy and exacerbates cardiac dysfunction.[43–45]

JNK, a member of the mitogen-activated protein kinase (MAPK) family, is activated in response to stress, such as MI/R, in the heart and brain. The JNK-dependent pathway is an important pathological mechanism of MI/R injury and promotes ROS generation, mitochondrial dysfunction and cardiomyocyte death.[46] Importantly, DIL can decrease hypoxia-reoxygenation (H/R)-induced apoptosis through the inhibition of $JNK_1/SAPK_1$ in rat hepatocytes. On the other hand, DIL can also inhibit JNK activation and consequently decrease IL-1β-induced TGF-β1 production in human peritoneal mesothelial cells.[47] Our results were similar to those of the above study. We demonstrated that DIL

inhibited MI/R-induced JNK activation in both our in vivo and in vitro experiments. Song et al reported that activation of the JNK-Bnip3-mitophagy pathway is a novel mechanism for MI/R injury, and approaches targeting this pathway are expected to improve MI/R injury. Additionally, DUSP1 (also known as MAPK phosphatase 1, MKP1) is an antiapoptotic phosphatase that is mainly expressed in the heart.[48] Some reports have shown that DUSP1 can inhibit cell death, protect mitochondrial homeostasis, and inhibit cell migration and invasion through the PKA pathway. Noticeably, Jin et al reported that DUSP1 prevents MI/R injury by suppressing the JNK pathway and subsequently inhibiting excessive mitochondrial fission and Bnip3-mediated mitophagy.[48]

In the present study, we showed that DIL inhibits excessive mitophagy by regulating the DUSP1-JNK-BNIP3L/NIX pathway. We utilized inhibitors/activators of these specific signal transduction pathways. DUSP1 expression was significantly decreased, and JNK and BNIP3L/NIX expression were significantly increased in MI/R injury. However, these effects could be reversed by DIL, suggesting that DIL may regulate the DUSP1-JNK-BNIP3L/NIX pathway, subsequently inhibiting excessive mitophagy and ultimately protecting the myocardium against MI/R injury.

The present study has some limitations. Conducting a well-designed experimental program based on gene knockout models in vivo and in vitro is necessary to determine the precise underlying molecular mechanisms by which diltiazem hydrochloride reduces mitophagy in myocardial ischemia/reperfusion injury, which should be the focus of future studies.

Conclusion

In conclusion, MI/R injury is closely with the inhibition of DUSP1, leading to the activation of JNK and BNIP3L/NIX, which causes excessive mitophagy and cardiomyocyte death. Diltiazem hydrochloride protects against myocardial ischemia/reperfusion injury in a BNIP3L/NIX-mediated mitophagy manner in vivo and in vitro.

Data Sharing Statement

The current study's data are available from the corresponding author Wensheng Lu upon reasonable request.

Acknowledgments

We thank the Guangxi People's Hospital Laboratory Center for cooperating as partners.

Author Contributions

All authors made a significant contribution to the work reported, whether that is in the conception, study design, execution, acquisition of data, analysis and interpretation, or in all these areas; took part in drafting, revising or critically reviewing the article; gave final approval of the version to be published; have agreed on the journal to which the article has been submitted; and agree to be accountable for all aspects of the work.

Funding

This research was funded by the National Natural Science Foundation of China (82160052, 81560044, and 30860113 for Wensheng Lu).

Disclosure

The authors have no conflicts of interest to declare.

References

1. Hamm CW, Bassand J-P, Agewall S, et al. ESC guidelines for the management of acute coronary syndromes in patients presenting without persistent ST-segment elevation: the task force for the management of acute coronary syndromes (ACS) in patients presenting without persistent ST-segment elevation of the European society of cardiology (ESC). *Eur Heart J*. 2011;32(23):2999–3054. doi:10.1093/eurheartj/ehr236
2. Virani SS, Alonso A, Aparicio HJ, et al. Heart disease and stroke statistics-2021 update: a report from the American heart association. *Circulation*. 2021;143(8):e254–e743. doi:10.1161/CIR.0000000000000950
3. Daiber A, Andreadou I, Oelze M, Davidson SM, Hausenloy DJ. Discovery of new therapeutic redox targets for cardioprotection against ischemia/reperfusion injury and heart failure. *Free Radic Biol Med*. 2021;163:325–343. doi:10.1016/j.freeradbiomed.2020.12.026
4. Heusch G. Myocardial ischaemia-reperfusion injury and cardioprotection in perspective. *Nat Rev Cardiol*. 2020;17(12):773–789.

5. Moens AL, Claeys MJ, Timmermans JP, Vrints CJ. Myocardial ischemia/reperfusion-injury, a clinical view on a complex pathophysiological process. *Int J Cardiol*. 2005;100(2):179–190. doi:10.1016/j.ijcard.2004.04.013
6. He J, Liu D, Zhao L, et al. Myocardial ischemia/reperfusion injury: mechanisms of injury and implications for management (Review). *Exp Ther Med*. 2022;23(6):430. doi:10.3892/etm.2022.11357
7. Bai M, Zhang J, Chen D, et al. Insights into research on myocardial ischemia/reperfusion injury from 2012 to 2021: a bibliometric analysis. *Eur J Med Res*. 2023;28(1):17. doi:10.1186/s40001-022-00967-7
8. Hernandez-Resendiz S, Prunier F, Girao H, Dorn G, Hausenloy DJ. Targeting mitochondrial fusion and fission proteins for cardioprotection. *J Cell Mol Med*. 2020;24(12):6571–6585. doi:10.1111/jcmm.15384
9. Wilson DF. Oxidative phosphorylation: regulation and role in cellular and tissue metabolism. *J Physiol*. 2017;595(23):7023–7038. doi:10.1113/JP273839
10. Karwi QG, Uddin GM, Ho KL, Lopaschuk GD. Loss of metabolic flexibility in the failing heart. *Front Cardiovasc Med*. 2018;5:68. doi:10.3389/fcvm.2018.00068
11. Kulek AR, Anzell A, Wider JM, Sanderson TH, Przyklenk K. Mitochondrial quality control: role in cardiac models of lethal ischemia–reperfusion injury. *Cells*. 2020;9(1):214. doi:10.3390/cells9010214
12. Lemasters JJ. Selective mitochondrial autophagy, or mitophagy, as a targeted defense against oxidative stress, mitochondrial dysfunction, and aging. *Rejuvenation Res*. 2005;8(1):3–5. doi:10.1089/rej.2005.8.3
13. Stowe DF, Camara AK. Mitochondrial reactive oxygen species production in excitable cells: modulators of mitochondrial and cell function. *Antioxid Redox Signal*. 2009;11(6):1373–1414. doi:10.1089/ars.2008.2331
14. Ramkissoon A, Chaney KE, Milewski D, et al. Targeted inhibition of the dual specificity phosphatases DUSP1 and DUSP6 suppress MPNST growth via JNK. *Clin Cancer Res*. 2019;25(13):4117–4127. doi:10.1158/1078-0432.CCR-18-3224
15. Onishi M, Yamano K, Sato M, Matsuda N, Okamoto K. Molecular mechanisms and physiological functions of mitophagy. *EMBO J*. 2021;40(3):e104705. doi:10.15252/embj.2020104705
16. Palikaras K, Lionaki E, Tavernarakis N. Mechanisms of mitophagy in cellular homeostasis, physiology and pathology. *Nat Cell Biol*. 2018;20(9):1013–1022. doi:10.1038/s41556-018-0176-2
17. Kim I, Rodriguez-Enriquez S, Lemasters JJ. Selective degradation of mitochondria by mitophagy. *Arch Biochem Biophys*. 2007;462(2):245–253. doi:10.1016/j.abb.2007.03.034
18. Li L, Tan J, Miao Y, Lei P, Zhang Q. ROS and autophagy: interactions and molecular regulatory mechanisms. *Cell Mol Neurobiol*. 2015;35(5):615–621. doi:10.1007/s10571-015-0166-x
19. Chen Z, Zhou Q, Chen J, et al. MCU-dependent mitochondrial calcium uptake-induced mitophagy contributes to apelin-13-stimulated VSMCs proliferation. *Vascul Pharmacol*. 2022;144:106979. doi:10.1016/j.vph.2022.106979
20. Hamacher-Brady A, Brady NR, Logue SE, et al. Response to myocardial ischemia/reperfusion injury involves Bnip3 and autophagy. *Cell Death Differ*. 2007;14(1):146–157. doi:10.1038/sj.cdd.4401936
21. Wu H, Chen Q. Hypoxia activation of mitophagy and its role in disease pathogenesis. *Antioxid Redox Signal*. 2015;22(12):1032–1046. doi:10.1089/ars.2014.6204
22. Hanna RA, Quinsay MN, Orogo AM, Giang K, Rikka S, Gustafsson AB. Microtubule-associated protein 1 light chain 3 (LC3) interacts with Bnip3 protein to selectively remove endoplasmic reticulum and mitochondria via autophagy. *J Biol Chem*. 2012;287(23):19094–19104. doi:10.1074/jbc.M111.322933
23. Yang M, Linn BS, Zhang Y, Ren J. Mitophagy and mitochondrial integrity in cardiac ischemia–reperfusion injury. *Biochim Biophys Acta Mol Basis Dis*. 2019;1865(9):2293–2302. doi:10.1016/j.bbadis.2019.05.007
24. Chourasia AH, Tracy K, Frankenberger C, et al. Mitophagy defects arising from BNip3 loss promote mammary tumor progression to metastasis. *EMBO Rep*. 2015;16(9):1145–1163. doi:10.15252/embr.201540759
25. Sandoval H, Thiagarajan P, Dasgupta SK, et al. Essential role for Nix in autophagic maturation of erythroid cells. *Nature*. 2008;454(7201):232–235. doi:10.1038/nature07006
26. Fu XH, Chen CZ, Li S, et al. Dual-specificity phosphatase 1 regulates cell cycle progression and apoptosis in cumulus cells by affecting mitochondrial function, oxidative stress, and autophagy. *Am J Physiol Cell Physiol*. 2019;317(6):C1183–C1193. doi:10.1152/ajpcell.00012.2019
27. Song X, Li T. Ripk3 mediates cardiomyocyte necrosis through targeting mitochondria and the JNK-Bnip3 pathway under hypoxia-reoxygenation injury. *J Recept Signal Transduction Res*. 2019;39(4):331–340. doi:10.1080/10799893.2019.1676259
28. Zhang W, Zhang Y, Zhang H, Zhao Q, Liu Z, Xu Y. USP49 inhibits ischemia–reperfusion-induced cell viability suppression and apoptosis in human AC16 cardiomyocytes through DUSP1-JNK1/2 signaling. *J Cell Physiol*. 2019;234(5):6529–6538. doi:10.1002/jcp.27390
29. Chen C, Lu W, Wu G, et al. Cardioprotective effects of combined therapy with diltiazem and superoxide dismutase on myocardial ischemia–reperfusion injury in rats. *Life Sci*. 2017;183:50–59. doi:10.1016/j.lfs.2017.06.024
30. Ding WX, Yin XM. Mitophagy: mechanisms, pathophysiological roles, and analysis. *Biol Chem*. 2012;393(7):547–564. doi:10.1515/hsz-2012-0119
31. Katayama H, Kogure T, Mizushima N, Yoshimori T, Miyawaki A. A sensitive and quantitative technique for detecting autophagic events based on lysosomal delivery. *Chem Biol*. 2011;18(8):1042–1052. doi:10.1016/j.chembiol.2011.05.013
32. Seif AA. Nigella sativa attenuates myocardial ischemic reperfusion injury in rats. *J Physiol Biochem*. 2013;69(4):937–944. doi:10.1007/s13105-013-0272-5
33. Liu Y, Li X, Sun T, Tao L, Qian L. Pyroptosis in myocardial ischemia/reperfusion and its therapeutic implications. *Eur J Pharmacol*. 2024;971:176464. doi:10.1016/j.ejphar.2024.176464
34. Chen C, Chen W, Nong Z, Ma Y, Qiu S, Wu G. Cardioprotective effects of combined therapy with hyperbaric oxygen and diltiazem pretreatment on myocardial ischemia–reperfusion injury in rats. *Cell Physiol Biochem*. 2016;38(5):2015–2029. doi:10.1159/000445561
35. Crenesse D, Tornieri K, Laurens M, et al. Diltiazem reduces apoptosis in rat hepatocytes subjected to warm hypoxia-reoxygenation. *Pharmacology*. 2002;65(2):87–95. doi:10.1159/000056192
36. Zhou H, Hu S, Jin Q, et al. Mff-dependent mitochondrial fission contributes to the pathogenesis of cardiac microvasculature ischemia/reperfusion injury via induction of mROS-mediated cardiolipin oxidation and HK2/VDAC1 disassociation-involved mPTP opening. *J Am Heart Assoc*. 2017;6(3):e005328. doi:10.1161/JAHA.116.005328

37. Gurkar AU, Chu K, Raj L, et al. Identification of ROCK1 kinase as a critical regulator of Beclin1-mediated autophagy during metabolic stress. *Nat Comun*. 2013;4:2189. doi:10.1038/ncomms3189
38. Ni HM, Bockus A, Wozniak AL, et al. Dissecting the dynamic turnover of GFP-LC3 in the autolysosome. *Autophagy*. 2011;7(2):188–204. doi:10.4161/auto.7.2.14181
39. Foerster EG, Mukherjee T, Cabral-Fernandes L, Rocha JDB, Girardin SE, Philpott DJ. How autophagy controls the intestinal epithelial barrier. *Autophagy*. 2022;18(1):86–103. doi:10.1080/15548627.2021.1909406
40. Kumariya S, Ubba V, Jha RK, Gayen JR. Autophagy in ovary and polycystic ovary syndrome: role, dispute and future perspective. *Autophagy*. 2021;17(10):2706–2733. doi:10.1080/15548627.2021.1938914
41. Qin L, Wang Z, Tao L, Wang Y. ER stress negatively regulates AKT/TSC/mTOR pathway to enhance autophagy. *Autophagy*. 2010;6(2):239–247. doi:10.4161/auto.6.2.11062
42. Imazu T, Shimizu S, Tagami S, et al. Bcl-2/E1B 19 kDa-interacting protein 3-like protein (Bnip3L) interacts with bcl-2/Bcl-xL and induces apoptosis by altering mitochondrial membrane permeability. *Oncogene*. 1999;18(32):4523–4529. doi:10.1038/sj.onc.1202722
43. Turkieh A, El Masri Y, Pinet F, Dubois-Deruy E. Mitophagy regulation following myocardial infarction. *Cells*. 2022;11(2):199. doi:10.3390/cells11020199
44. Dorn GW 2nd, Kirshenbaum LA. Cardiac reanimation: targeting cardiomyocyte death by BNIP3 and NIX/BNIP3L. *Oncogene*. 2008;27(Suppl 1):S158–67. doi:10.1038/onc.2009.53
45. Birse-Archbold JL, Kerr LE, Jones PA, McCulloch J, Sharkey J. Differential profile of Nix upregulation and translocation during hypoxia/ischemia in vivo versus in vitro. *J Cereb Blood Flow Metab*. 2005;25(10):1356–1365. doi:10.1038/sj.jcbfm.9600133
46. Chambers JW, Pachori A, Howard S, Iqbal S, LoGrasso PV. Inhibition of JNK mitochondrial localization and signaling is protective against ischemia/reperfusion injury in rats. *J Biol Chem*. 2013;288(6):4000–4011. doi:10.1074/jbc.M112.406777
47. Fang CC, Yen CJ, Chen YM, et al. Diltiazem suppresses collagen synthesis and IL-1beta-induced TGF-beta1 production on human peritoneal mesothelial cells. *Nephrol Dial Transplant*. 2006;21(5):1340–1347. doi:10.1093/ndt/gfk051
48. Jin Q, Li R, Hu N, et al. DUSP1 alleviates cardiac ischemia/reperfusion injury by suppressing the Mff-required mitochondrial fission and Bnip3-related mitophagy via the JNK pathways. *Redox Biol*. 2018;14:576–587. doi:10.1016/j.redox.2017.11.004